Annals of Biomedical Engineering, Vol. 37, No. 3, March 2009 (© 2008) pp. 542–551
DOI: 10.1007/s10439-008-9623-8

Volume Ordering for Analysis and Modeling of Vascular Systems

M. MARXEN,[1] J.G. SLED,[2,3] and R.M. HENKELMAN[2,3,4]

[1]Rotman Research Institute, Baycrest Centre for Geriatric Care, 3560 Bathurst St., Toronto, ON M6A 2E1, Canada; [2]Department of Medical Biophysics, University of Toronto, Toronto, Canada; [3]Hospital for Sick Children – Mouse Imaging Centre, Toronto, Canada; and [4]Sunnybrook Health Sciences Centre, Toronto, Canada

(*Received 29 October 2007; accepted 12 December 2008; published online 24 December 2008*)

Abstract—Morphological characteristics of vascular systems are commonly presented in terms of Strahler order because the logarithms of quantities such as vessel diameter and length are often linearly related to Strahler order. However, the ability to interpret Strahler order geometrically or physiologically is compromised because the precision of the order number is limited to integer values. This limitation is overcome by the volume ordering scheme, in which volume order number is defined as the logarithm of the estimated perfused tissue volume for each vascular segment. While Strahler and volume order numbers are equivalent for completely symmetrical branching trees, they deviate in the presence of asymmetries. The physiology-based definition of volume ordering offers benefits in the analysis of vascular design, fractal characterization of vascular systems, and blood flow modeling. These benefits are illustrated based on arterial kidney data that show a linear relationship of logarithmic vessel diameter and conductance as a function of both Strahler order and volume order with differing proportionality constants, which are expected to depend on the branching characteristics of the particular organ investigated.

Keywords—Vessel ordering, Strahler ordering, Fractals, Vascular morphology, Tree topology, Murray's law, Arterial kidney vasculature, Three-dimensional flow modeling, MicroCT imaging.

INTRODUCTION

A common way of characterizing a particular vascular system is to examine its geometric parameters as a function of vessel order number. In the Strahler scheme,[3,16] arterioles are usually assigned order 1 or 0 and subsequent vessel segments are assigned the maximum order number of the daughter branches or the next higher integer number if the orders of both daughter branches are the same (see Fig. 1). 'Segments' denote here the connections between subsequent branching points of the tree structure. The Strahler scheme has been particularly useful in the morphological analysis of vascular trees because the logarithms of quantities such as vessel diameter and length have been found to be linearly dependent on order number.[12] However, a quantitative and comparative study of the proportionality constants (slopes) of these relationships is difficult because the geometrical and physiological interpretation of Strahler order number is lost due to the cumulative effect of limiting order precision to integer numbers at each bifurcation. For example, it can easily be seen that the addition of an arbitrary number of subtrees has no effect on the Strahler order numbers of the original tree as long as the order of the root of the subtree is less than the order of the branch it is added onto.

Strahler order was originally designed to classify segments of a riverbed in terms of how much land was being drained.[16] In a similar fashion, it appears reasonable to classify vascular segments in terms of how much tissue volume they perfuse. However, given the above limitations, the numerical relationship between Strahler order number and drained land or perfused tissue is unknown. This loss of information can be avoided if non-integer order numbers are permitted in the recursive ordering procedure. This idea is implemented in the volume ordering scheme (see Fig. 1), which defines volume order as the logarithm to base 2 of the estimated perfused volume and was proposed by Marxen and Henkelman[5] in 2003. Note that this definition of the volume order number leads to the same numbering as Strahler ordering for symmetric trees in which the order of two daughter branches are always the same (and integer). It should also be noted that volume ordering can be applied in any situation in which Strahler ordering is possible. Both systems only assume dichotomous branching and some method of ordering the terminal branches of the tree.

Address correspondence to M. Marxen, Rotman Research Institute, Baycrest Centre for Geriatric Care, 3560 Bathurst St., Toronto, ON M6A 2E1, Canada. Electronic mail: mmarxen@rotman-baycrest.on.ca

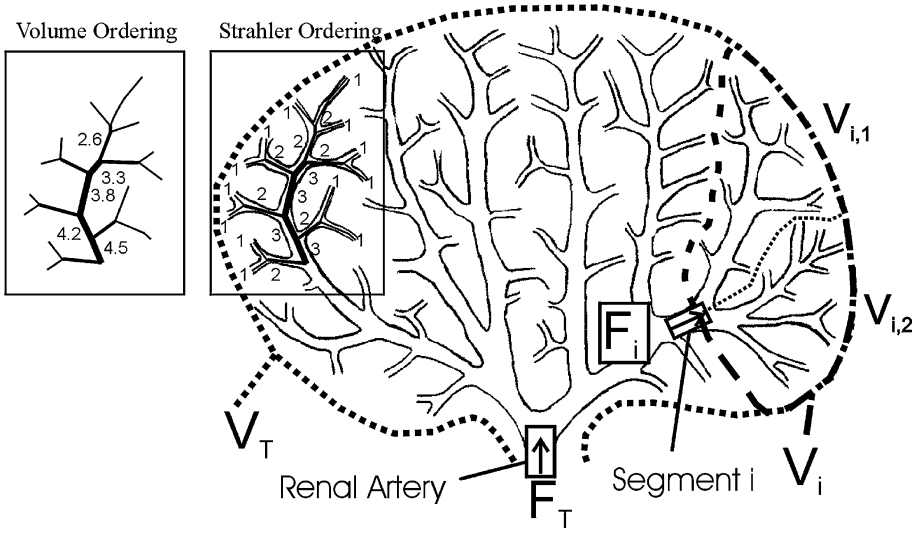

FIGURE 1. This 2D schematic of the kidney arterial tree illustrates volume ordering in contrast to Strahler ordering. On the left side of the figure, Strahler ordering is compared with volume ordering for a subtree of the kidney. Volume orders are only explicated when different from the corresponding Strahler order. For simplicity, we have assumed here that all terminal segments of the arterial tree have order number 1 in both ordering schemes. The Strahler method (see section "Introduction") ignores small side branches and leads to the same order number for vessel segments that supply vastly different volumes of tissue. In contrast, volume order number, defined as $\log_2$(designated fed volume), accounts for the added volume at each branching. The designated fed volume of any non-terminal vessel V_i equals the sum of the designated fed volumes of the two daughter branches $V_{i,1} + V_{i,2}$ and also the sum of the designated fed volumes of all terminal vessels downstream of segment *i*. Local perfusion $Perf_i$ is approximated by the blood flow F_i through segment *i* divided by the designated fed volume V_i. Average or total Perfusion $Perf_T$ equals F_T/V_T, where F_T is the total blood flow through the renal artery and V_T is the total perfused volume.

In this paper, we examined arterial kidney data with the hypothesis that similar log-linear relationships for vascular dimensions that were reported previously for Strahler ordering also exist for volume ordering, which would imply a linear relationship between volume order and Strahler order. Based on the discovered proportionality constants, which differ between the ordering schemes, we demonstrate how volume ordering benefits the quantitative analysis and reconstructive modeling of vascular systems.

MATERIALS AND METHODS

Morphological analyses of four kidney arterial trees (2 kidneys of 2 CD1 mice and 2 kidneys of a Wistar rat) were conducted. The kidneys were perfused with the radiopaque, polymerizing silicone rubber compound Microfil (4 mL MICROFIL MV122, 5 mL high-viscosity (HV) diluent, and 0.45 mL curing agent) at pressure levels that guaranteed almost complete filling of the arterial tree but no passage of contrast material into venous vessels. Perfusion pressures were approximately, 160 mmHg in mice and 130 mmHg in rat. Three-dimensional images of the excised kidneys with voxel (volume elements) sizes of 22 μm (mice) and 38 μm (rat) were obtained using the General Electric Medical Systems MS8 microCT (80 kVp tube voltage, and 324 mAs total exposure for mice and 486 mAs for the rat specimen). The Animal Care Committee of Sunnybrook & Women's College Health Sciences Centre approved all animal procedures. A previous publication[7] describes the sample preparation and imaging procedures (see Fig. 2) in more detail.

Information on vascular topology, vessel segment diameter and length were obtained using largely automated computer code.[15] Segment conductance C as a function of vessel diameter d, segment length l (both in μm), and blood viscosity v is calculated using Poiseuille's law for laminar flow and the expression given by Pries *et al.*[14] for the viscosity of blood *in vivo* assuming a plasma viscosity v_0 of 9×10^{-6} mmHg s and a discharge hematocrit of 0.45:

$$C = \frac{\pi d^4}{128 v l} \text{ where}$$

$$v(d) = v_0 \left[1 + (\eta - 1)\left(\frac{d}{d - 1.1}\right)^2\right]\left[\frac{d}{d - 1.1}\right]^2 \text{ and}$$

$$\eta(d) = 6\exp(-0.085d) + 3.2 - 2.44\exp(-0.06d^{-0.6645}) \quad (1)$$

Strahler and volume ordering was performed for all specimens. As an estimation of the tissue volume perfused by each segment, a designated fed volume V is determined for all terminal ends of the vascular tree.

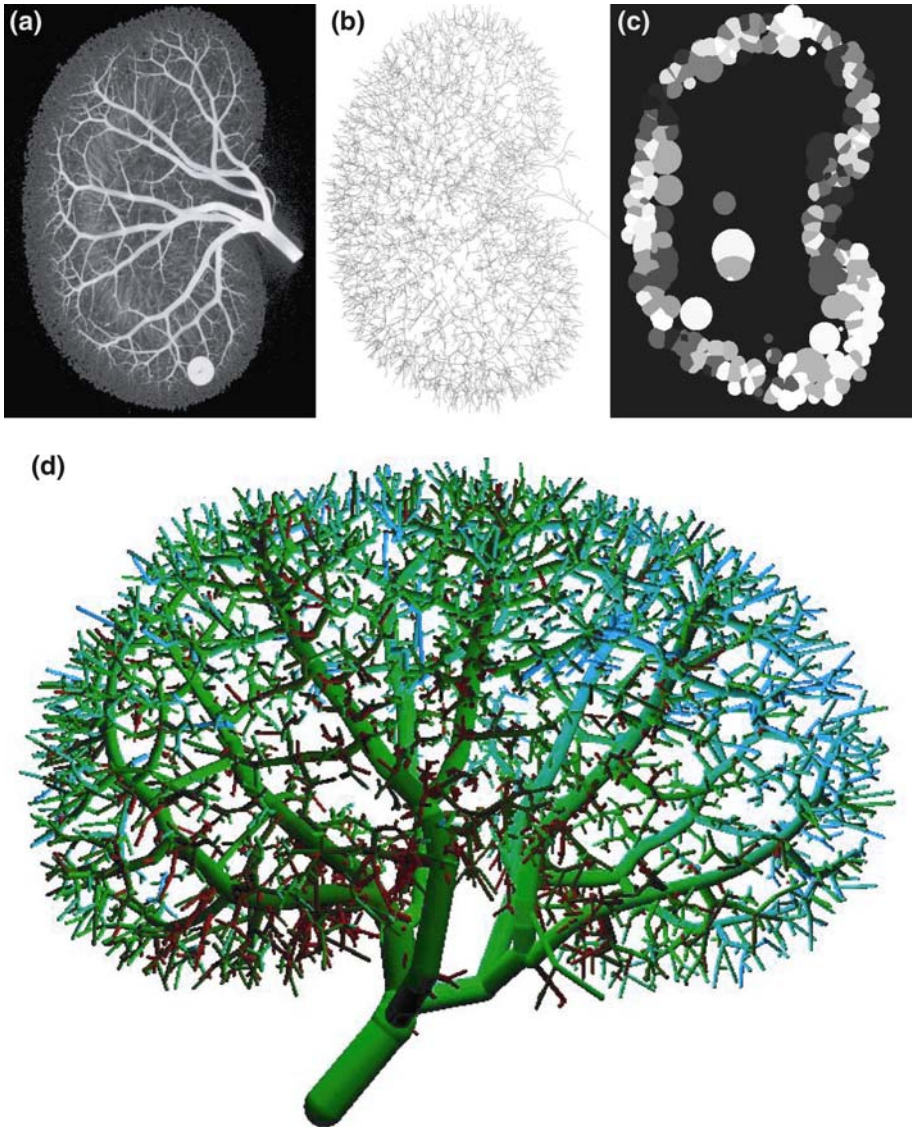

FIGURE 2. Processing steps illustrated in rat 1 starting with the microCT image (maximum intensity projection) in (a) to an eventual cylinder model of the arterial tree (d) with segments color-coded according to the modeled perfusion level with green being average perfusion, light blue half the average perfusion, and dark red double the average perfusion. The long axis of the kidney is approximately 2 cm. Arterioles down to about 80 μm in diameter could be resolved. After a threshold-based segmentation of the vessels, a skeletonization (b) is performed, which is used to determine the location of branching points and vessel diameters. To perform volume ordering, a modified nearest-neighbor approach with a distance threshold is taken to assign designated fed volumes to terminal branches of the tree. (c) is a coronal slice through the labeled fed volume map. Regions of different gray scale are the intersection of the slice plane with the fed volumes of terminals that may end outside this plane. The black space is not considered perfused volume.

The designated fed volumes for all non-terminal segments are simply the sums of the designated fed volumes of all downstream terminal segments.

To determine the terminal designated fed volumes, two questions need to be resolved: (1) Which voxels belong to the total perfused volume and (2) What is the appropriate terminal vessel segment that each perfused voxel should be associated with? First of all, we will state that our goal was to include only the kidney cortex as perfused volume (see section "Discussion"). Given, however, that our data supplies no contrast between the kidney cortex and the medulla or embedding medium, we chose the following answers to these questions. In our approach, the second question is addressed first (see Fig. 3). For each voxel v, its Euclidian distance $s_{v,j}$ to each terminal end j of the vascular tree is calculated. Each of these distances is now weighted by the inverse diameter $1/d_j$ of each terminal vessel segment to account for the fact that some terminal segments in the data set have a much

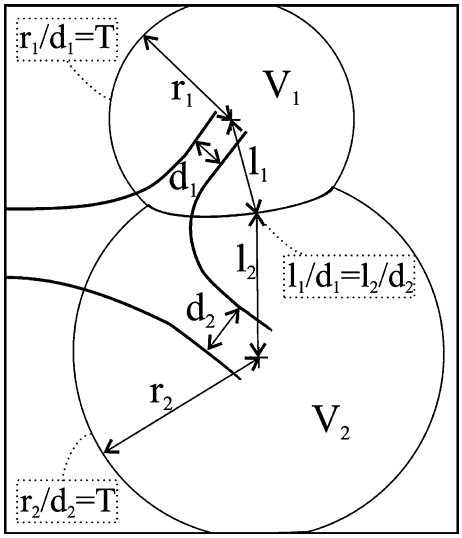

FIGURE 3. An illustration of how designated fed volumes are determined for two neighboring terminal vessel segments. The designated fed volume of a terminal vessel is obtained by adding up all nearest-neighbor voxels within the image with a weighted distance r_j/d_j to the nearest terminal endpoint smaller than a threshold value T (see text for details). Distances are weighted with the inverse segment diameter d_j to account for the fact that larger vessels are expected to feed a larger volume. At the interface of two perfusion volumes $l_1/d_1 = l_2/d_2$. The threshold value T determines the boundary of the total perfused volume and is chosen as the minimum value that maintains connectivity between all terminal designated fed volumes.

larger diameter than others and are expected to feed a larger volume. Now the voxel v is assigned to the terminal j' with the minimum $s_{v,j}/d_j$. To answer the first question now, a threshold value T for $s_{v,j'}/d_{j'}$ was introduced, beyond which a voxel was no longer considered perfused. We have chosen T to be the minimum value that maintains connectivity between all terminal volumes:

$$T = \max_i \left\{ \min_{j \neq i} \left\{ \frac{D_{ij}}{d_i + d_j} \right\} \right\}, \tag{2}$$

where D_{ij} is the Euclidean distance between the terminal endpoints i and j. d_i and d_j are the respective segment diameters. The shape of the resulting volume resembles the kidney cortex (see Fig. 2c). As the value of T is relatively high, holes within his structure are very infrequent.

Volume order number U_{vol} is now defined by the equation

$$U_{\text{vol}} \equiv \log_2 \left[\frac{V}{V_0} \right], \tag{3}$$

where V_0 was chosen such that U_{vol} equals 1 for a designated fed volume of $(100\ \mu\text{m})^3$.

To determine the Strahler order of all terminal segments within the reconstructed arterial trees, an iterative approach was taken to generate diameter ranges for each Strahler order. The idea is similar to the diameter-defined Strahler ordering scheme as proposed by Kassab *et al.*[3] but only terminal segments are assigned Strahler orders based on diameter. All other segments are ordered according to the Strahler rules (see section "Introduction" and Fig. 1). A similar approach was also taken by Nordsletten *et al.*[10] In our work, the median of all terminal segment diameters is taken as the maximum diameter for Strahler order 1. Consequently, half of all terminal segments are of order 1 while the order of the remaining segments is still to be determined. Now Strahler orders can be assigned to all segments that have downstream subtrees with defined order numbers. The resulting order 2 vessels are used to calculate the new maximum diameter for order 1 vessels as the midpoint between the mean diameter of order 1 vessels and the mean diameter of order 2 vessels. In the next iteration, the maximum diameter of order 2 vessels is defined and some terminal vessels can be assigned order 2. Iterations are continued until order numbers have been assigned to all terminal segments. Note here that slopes in terms of diameter-defined Strahler ordering are nearly identical with those in the Strahler scheme.

Geometrical parameters of each vascular tree were fitted with the equation

$$\log_2(f) = L + bU, \tag{4}$$

where f represents vessel segment diameter, length, and conductance, and U the order number. Only data for volume orders above 7 in mice and above 12 in rats, for which the parameter distributions appeared complete and not limited by the resolvable vessel size, are used for fitting. Terminal ends were excluded from the fits to minimize a bias effect due to the diameter weighting in the calculation of the terminal fed volumes. To estimate whether Eq. (4) actually describes the data well, a reduced χ^2 value of the least square fit to the data was estimated. The squared deviations of each data point from the regression line were weighted by the inverse of the mean squared deviation from the regression line of data points that would round to the same integer volume order.[13] The Pearson correlation coefficient R is stated. The thresholds for significant differences (p values) between correlation coefficients were determined by estimating the probability distributions of the correlation coefficients using the bootstrap algorithm.[13] One thousand simulated data sets were drawn randomly with replacement from the original data for these estimates. This approach was also used to determine standard deviations for the fitted parameters.

As an application example for volume ordering, flow and subtree conductance are quoted below based on a

model detailed in Marxen *et al.*[4,6] Briefly, constant inflow pressure (non-pulsatile flow) at the level of the renal artery, constant outflow pressure at the level of the capillaries, and laminar blood flow are assumed. To compute subtree conductances down to the outflow level, we estimated the conductance of unresolved terminal subtrees by numerically extending each terminal end of the measured vascular tree. Continued branching with the asymmetry parameter δ is performed for segments with volume order >4 (6 in rat). We define the branching asymmetry parameter $\delta \equiv V_1/(V_1 + V_2)$, where V_1 and V_2 are the tissue volumes being fed by the daughter branches of a vessel bifurcation ($0 < \delta < 1$). Using this definition, δ is symmetric about 0.5. In the simulation, δ was chosen from a normal distribution with a mean of 0.5 and a standard deviation equal to the measured value for bifurcations of vessels with integer volume order 7 (10 in rat). A conductance was assigned to each added segment based on its volume order. The $\log_2$(conductance) of the added segments was taken from a normal distribution with mean value according to the fitted fractal law (Eq. 4) and with a standard deviation equal to the measured value for vessel segments with volume order 7–8 (12–13 in rat). With the knowledge of all subtree conductances, calculating flow in each segment is straightforward.

RESULTS

Figure 4 illustrates the dependence of vessel segment length, segment diameter, and segment conductance on volume order for mouse 1. Similar analyses were performed for the other three specimens. The logarithm of individual segment length (Fig. 4a) correlates poorly with volume order as well as with Strahler order ($R < 0.11$ for all specimens) and no fitting results are reported. Approximately one thousand segments from more than 2000 detected segments in mouse and more than 7000 detected segments in rat were fitted in each case. Terminal segments are not fitted and are marked with crosses in the plots. The difference in the fitting parameters is negligible if the terminal segments are included in the fit.

The χ^2-values and correlation coefficients indicate that the fitting model works well for segment diameter and conductance. The fitting results for all four specimens are summarized in Table 1, which also contains results for subtree conductance. Subtree conductance data is only mentioned here for readers with an interest in vascular design and flow modeling and as an application example of volume ordering (see section "Discussion").

Figure 5 illustrates the relationship between volume order and Strahler order. The linear regression line

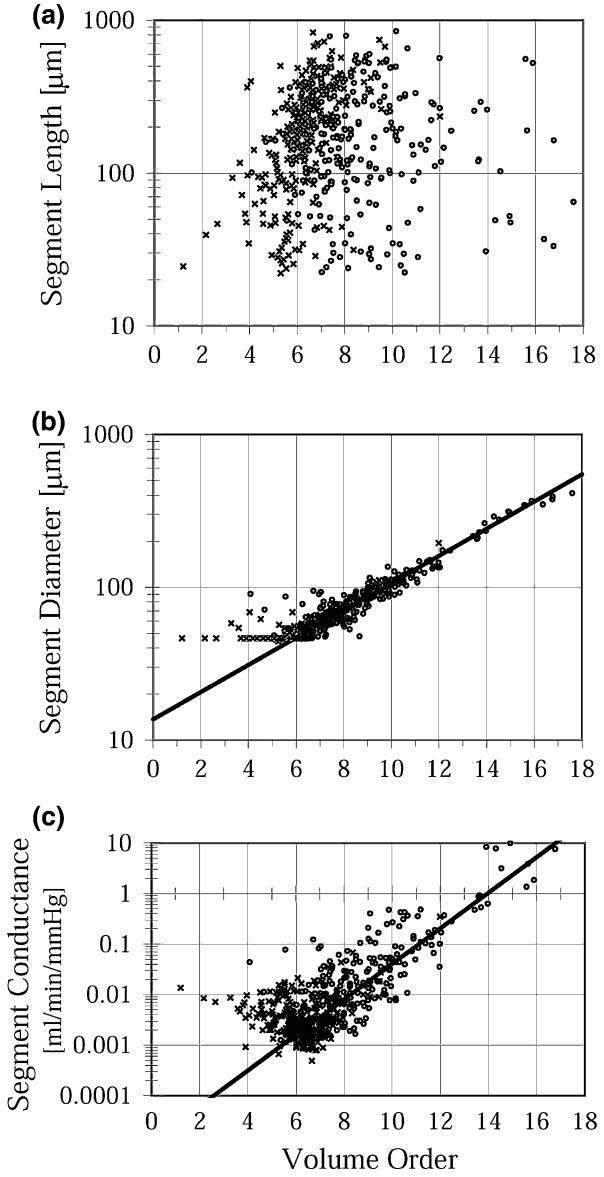

FIGURE 4. Vessel segment length (a), diameter (b), and inferred conductance (c) are plotted versus volume order for mouse 1. No correlation is observed for segment length versus volume order. χ^2 fits are shown for segment diameter and conductance measurements for volume orders above 7 (see text). The fitted parameters are summarized in Table 1. For clarity, only 25% of all data points are displayed. × indicates terminal segments, which are not included in the fits.

relating the two in Fig. 5a has a slope of 1.68 ($R = 0.92$). The slopes for mouse 2, rat 1, and rat 2 were 1.87, 1.66, and 1.70, respectively. The correlation between the logarithm of diameter and binned volume order (Fig. 5b, $R = 0.94$) is only slightly higher ($p < 0.02$) than the correlation with Strahler order (Fig. 5c, $R = 0.91$). Being not only integer valued, volume ordering has an intrinsic advantage over Strahler ordering. Thus, volume orders were binned in

TABLE 1. Fitting results for segment diameter *d*, conductance *C*, and subtree conductance C_s.

(a) Segment diameter d (in μm)

Specimen	L_d	b_d	χ^2	R
Mouse 1	3.76 ± 00.02	0.297 ± 0.002	1.11	0.96
Mouse 2	3.68 ± 0.03	0.311 ± 0.003	1.02	0.94
Rat 1	3.41 ± 0.03	0.302 ± 0.002	1.01	0.97
Rat 2	3.37 ± 0.04	0.301 ± 0.003	1.03	0.95

(b) Segment conductance C (in mL/min/mmHg)

Specimen	L_C	b_C	χ^2	R
Mouse 1	−15.9 ± 0.1	1.14 ± 0.02	1.02	0.90
Mouse 2	−16.8 ± 0.2	1.22 ± 0.02	1.00	0.88
Rat 1	−18.7 ± 0.3	1.21 ± 0.02	1.02	0.89
Rat 2	−17.8 ± 0.3	1.12 ± 0.02	1.02	0.87

(c) Subtree conductance C_s (in mL/min/mmHg)

Specimen	L_{Cs}	b_{Cs}	χ^2	R
Mouse 1	−16.23 ± 0.02	0.822 ± 0.002	0.99	0.99
Mouse 2	−17.26 ± 0.04	0.879 ± 0.003	1.02	0.99
Rat 1	−18.29 ± 0.04	0.870 ± 0.005	1.00	0.99
Rat 2	−17.40 ± 0.05	0.810 ± 0.003	1.21	0.99

Model equation: $\log_2(p) = L + bU_{vol}$. Standard deviations, the reduced χ^2-value, and the correlation coefficient R are given.

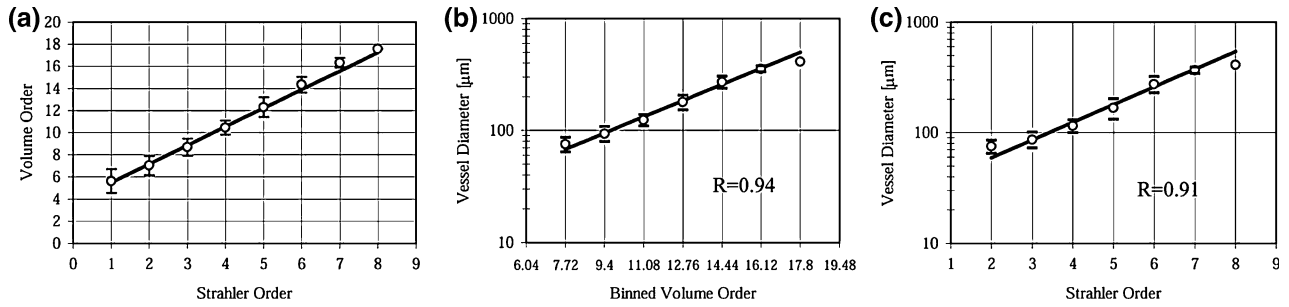

FIGURE 5. Comparing the Strahler and volume ordering schemes for mouse 1: the first panel shows the range of volume orders for different Strahler orders (a). The least-square regression line has a slope of 1.68. The other two panels demonstrate the relationships between vessel diameter and binned volume order (b) and vessel diameter and Strahler order (c). Binning brings the resolution of the volume ordering data down to the same level as for Strahler ordering. Linear regression fits of the logarithm of diameter are shown. As expected the ratio of the slopes of the logarithmic data (base 10) in (b) of 0.089 and in (c) of 0.15 equals approximately 1.68. The correlation coefficient *R* of vessel diameter versus binned volume order is slightly higher than for vessel diameter versus Strahler order. All error bars indicate ±1 standard deviation. Note that at low order numbers many more points contribute to the fits.

Fig. 5b with a bin width equal to the above slope for a fair comparison. While the improvement in correlation using volume order is small, it is consistent for all specimens and also for the logarithm of segment conductance versus order numbers, giving a consistent preference to volume ordering.

DISCUSSION

It is a limitation of this study, that we can only present kidney data of mice and rats with limited resolution. Future studies in other organs, such as the lungs and hearts, in other animals and humans and ideally with the capability of resolving the smallest arterioles are desirable. The kidney was chosen for this study because of its obvious tree-like architecture on the probed vascular scales and experimental considerations. At these scales, the vast majority of terminals end in the cortex region. The medulla region, which is 4- to 10-fold less perfused than the cortex,[11] is ignored in this study. The medulla is perfused by very small diameter vessels 'dipping down' from the cortex. Because of this particular vascular architecture, it is

impossible to assign voxels in the medulla to a particular terminal of the branching tree. Within this study, the medulla may be regarded as a small, spatially homogeneous additional sink for blood delivered to the cortex, which would result in an inconsequential scaling factor for the designated fed volumes.

Our methodology of estimating the perfused tissue volume might be criticized. However, the advantages of the volume ordering procedure over Strahler ordering discussed below remain even when a simplistic approach of assigning order 1 to all terminal vessel segments is taken, which increases the fitting parameters by approximately 10%. This is indicated by the slopes of volume order versus the simplistic volume order being 1.01, 1.11, 1.06, and 1.07 for mouse 1/2 and rat 1/2, respectively. At small scales, any estimate of the perfused tissue volume is bound to be inaccurate due to measurement limitations and the fact that a precise location of the perfusion boundaries does not exist physiologically. Any space-dividing procedure offers here the advantage that a misplacement of the boundary between neighboring perfusion volumes affects the neighboring volumes in a compensatory manner. This anti-correlation reduces the relative error of volume estimates more rapidly with aggregation as compared with procedures that introduce random volume errors such as assigning the same perfusion volume to all terminals.

With microCT and a field-of-view covering an organ completely, one will inevitably be plagued with inadequate resolution to resolve the smallest vessels. Under these conditions, an ordering scheme should have the property that it will remain unchanged even if higher resolution data becomes available. Excluding extreme cases of non-uniform vascular design (for example, in response to vascular occlusion), volume ordering has this property with a reduction of boundary errors as resolution is increased. For Strahler ordering, unvalidated assumptions are required to determine terminal orders in incomplete trees (see section "Methods").

The experimental results in the four kidneys indicate clearly that the relationship between the logarithms of vessel segment diameter and conductance and volume order is well described by the linear equation (4). It is demonstrated that the correlation with volume order is at least as strong as with Strahler order. As expected in this case, Strahler and volume order were found to be linearly related with slopes ranging from 1.66 (rat 1) to 1.87 (mouse 2). These values also represent the ratio of slopes of the vascular parameters in Eq. (4) between Strahler order and volume order.

These results are the first experimental confirmation that Strahler order is linearly related to the logarithm of the fed volumes or volume order. The above slopes are the first quantification of this relationship. Neither the linearity, nor the value of the slope can be assumed *a priori* as one can easily construct a tree in which Strahler and volume order would not be related linearly (see simulations below). A disconnect between Strahler order and fed volume may, for example, explain the strange finding by Nordsletten *et al.*[10] that arteries and veins often run parallel in kidneys, but that the Strahler order of the artery are two orders below the paired vein. Knowledge of fed volumes or volume ordering is essential for perfusion modeling and aids in the interpretation of morphological scaling laws, which will become more apparent in the paragraphs below.

Figure 6 demonstrates how Strahler order and volume order are related in simulated tree structures with constant asymmetry (defined in Fig. 6). For symmetric trees, the ordering schemes are identical. However, as asymmetry increases, Strahler order increases more slowly than volume order because Strahler ordering has the tendency to ignore small side branches. As asymmetry in organs such as the heart can be expected to be larger than in kidneys or lungs, Strahler and volume orders may differ even more strongly in studies of different organs than in this study of kidneys only.

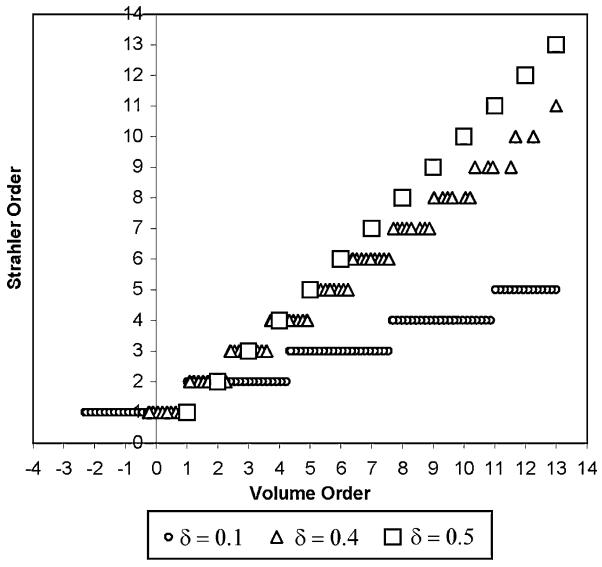

FIGURE 6. Strahler order as a function of volume order for three computer simulated branching trees with constant branching asymmetry. The branching asymmetry parameter δ is defined as $\delta \equiv V_1/(V_1 + V_2)$, where V_1 and V_2 are the designated fed volumes of the daughter branches. Trees are simulated with $\delta = 0.5$ (symmetric branching), 0.4 and 0.1. It can be seen that the range of volume orders that corresponds to each Strahler order increases with branching asymmetry. Strahler orders are approximately linearly related to volume order for constant values of δ but the slope of the relationship decreases with increasing asymmetry.

Note that negative volume orders arise at the last branching for asymmetric trees because the last split produces now smaller volumes than arbitrarily assigned order 0.

In the interpretation of vascular scaling laws, the language of fractals is often employed. Using Eq. (3), Eq. (4) can be transformed into the power law

$$f(V) = f(V_0)\left(\frac{V}{V_0}\right)^b. \tag{5}$$

The existence of a power law implies that f is self-affine[1] meaning that the ratio between its value measured at a scale nV and the value measured at the scale V equals a constant $k = n^b$, which is independent of V and characteristic for the property of interest:

$$\frac{f(nV)}{f(V)} = k. \tag{6}$$

We refer to the function f in Eqs. (5) and (6) here as fractal because of the self-affinity and because the designated fed volume V can be regarded as a measure of geometric scale. And for volume ordering, Eq. (4) can also be regarded as fractal because n is, by definition, equal to 2 as volume order increases by 1, and the relationship to scale is therefore known. For Strahler ordering, however, the value of n equivalent to an order increase of 1 may be different for different specimens, and k-values would, therefore, not be comparable. In the case that n is equivalent to an increase in Strahler order of 1, Eq. (6) is known as Horton's law and has been observed for vessel number, diameter, and length in a number of organs.[12] We suggest that Horton's laws should be reexamined using the volume ordering approach to generate comparable parameters k.

Due to the direct relationship between volume order and the designated fed volume, the interpretation of slopes in Eq. (4) is clear. For example, the observation of a power law for vessel diameter $d \propto V^{b'}$ combined with the additivity of daughter volumes $V = V_1 + V_2$ would imply that $d^{1/b'} = d_1^{1/b'} + d_2^{1/b'}$. Murray and others suggested that the sum of the cubes of the vessel diameters is conserved at bifurcations to minimize the biological work required to maintain a required blood flow.[9] Murray's law would therefore predict $1/b' = 3$. This would explain the observed exponent $b_d \approx 0.3$ to within about 10% error (see Table 1). Our measurements of b_d are smaller than the results of other researchers, who estimated a value of 1/2.7 in human[17] and 1/2.5 in pig[19] kidney. We believe, however, that our estimation of b_d is robust given that it includes all branches above a certain volume order and does not rely on calculating Murray's exponent for individual bifurcations, which is known to result in wide distributions for the exponent.[17] The recent study by Nordsletten *et al.*[10] found that an exponent of 3.0 was consistent with data in a rat kidney but an optimal fit of the exponent was not presented.

The observed exponent b_C for vessel conductance C ranges from 1.13 to 1.26 and is governed by $4{\cdot}b_d \approx 1.2$ through Poiseuille's law (Eq. 5) since segment length is almost independent of scale. It is sometimes argued based on space-filling arguments[2,8,18] that segment length should scale with $b = 1/3$. This is not supported for kidney by our data and neither by the data of Nordsletten *et al.*[10]

Volume ordering has additional advantages when modeling blood flow. Figure 7 displays flow and subtree conductance in a kidney arterial tree according to a model described in the "Methods" section. Quoted measurement values serve as examples only. As the designated fed volume doubles from one volume order to the next, it is expected for homogeneous perfusion that the flow of blood would also double. Accordingly, the slope of $\log_2$(flow) as a function of volume order is expected to be close to 1. The fitted value was 1.03. Similarly, it is expected that as the designated fed volume doubles subtree conductance should not quite double because a higher order connecting branch would add additional resistance. The slope of $\log_2$(subtree conductance) as a function of volume order is, therefore, expected to be less than 1. Given that metabolic rate in mammals has been observed[18] to scale with body mass to the power of 0.75, a similar exponent may be expected for subtree conductance. The fitted value was 0.822 in mouse 1. These plausibility arguments are not possible with Strahler ordering.

For computer-generated vascular trees, matching morphological statistics based on volume ordering promises closer resemblance to reality because volume ordering does not suffer the same information loss as Strahler ordering. Strahler ordering looses any sense of perfused volumes, which are essential for perfusion modeling. This loss of information occurs in the same way for the Strahler variant diameter-defined Strahler ordering,[3] which is a re-numbering of Strahler orders such that diameter ranges of different orders no longer overlap. The correlation of volume order and diameter-defined Strahler order is not significantly higher than with standard Strahler ordering, and the associated slopes are not significantly different, either.

In conjunction with diameter-defined Strahler order, the idea of a statistical connectivity matrix[3] was introduced to describe branching characteristics within a vascular tree structure. Using volume orders, a statistical description of branching asymmetry (as defined in Fig. 6) could serve a similar purpose with the advantage that it would only be a one-dimensional (statistical) function of parental volume order. For

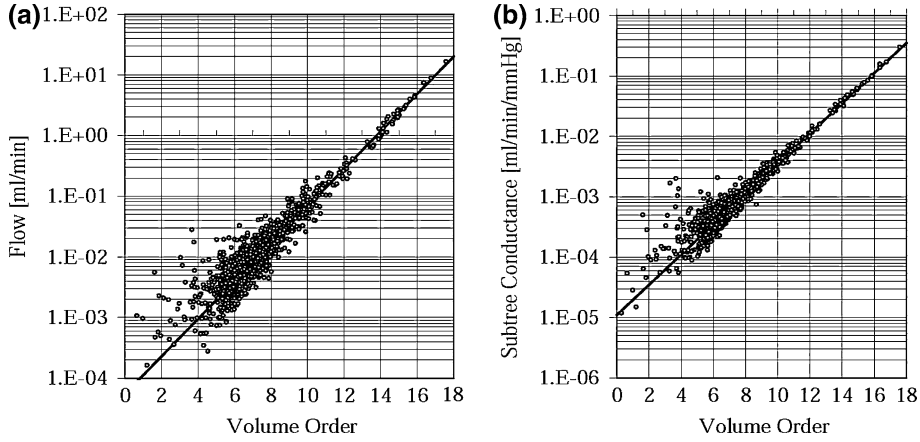

FIGURE 7. Extrapolation of segment conductances down to the level of the capillary bed is used to estimate subtree conductance and flow. Flow (a) and subtree conductance (b) are plotted as a function of volume order. Minimum χ^2 fits for volume orders above 7 are also shown. The slopes of the fitting lines for $\log_2$(flow) and $\log_2$(subtree conductance) are 1.03 and 0.822, respectively.

(diameter-defined) Strahler orders, the orders of daughter branches are only restricted to be smaller or equal than the parent order but are not uniquely related. This ambiguity is unnecessary and avoided in the volume ordering scheme through the additivity of the designated fed volumes.

Having discussed now at length how volume ordering can add another layer of meaning to the description of vascular morphology, it should be noted that it is still only an incomplete picture of the complexity of a real vascular system and does not describe vascular systems with collateral vessels. We believe that vessel ordering is a useful approach to highlight key design features of vascular systems. In fact, judging the similarity between different vascular systems is very hard without some concept of equivalent vessels. However, an order number is insufficient to capture all affecters of vascular design. For any natural vascular system, a significant variability of vascular parameters around the fractal laws is expected for any ordering technique, even ignoring measurement errors. This variability certainly deserves further studies, which is, however, beyond the scope of this paper. In addition, capturing the details of vessel arrangement in three-dimensional space and the effects of metabolic heterogeneity, for example, will require concepts beyond geometry-based vessel ordering.

CONCLUSION

The experimental results in arterial kidney vasculature demonstrate that logarithmic vessel segment diameter and conductance are linearly dependent on both Strahler and volume order with differing slopes. Volume ordering is the preferred ordering scheme for quantitative studies of these slopes because only volume ordering is well defined in terms of a physiologically relevant geometric scale. Fractal parameters can be quantitatively compared and information loss as it occurs in Strahler ordering is avoided. The relationship between Strahler and volume ordering was found to be approximately linear but with differing slopes for different specimens and for simulations with different branching asymmetry, which indicates that a universal relationship between Strahler order and the perfused tissue volume does not exist. A number of examples were given showing how meaningful interpretations of morphological data can be obtained through volume ordering that would not have been possible with Strahler ordering.

We recommend the use of volume ordering for future morphological studies and believe that it would be beneficial to generate data bases of fractal parameters based on volume ordering for comparative studies of different types of organs, species, and pathologies.

ACKNOWLEDGMENTS

This research is supported by the Canadian Institutes of Health Research and the National Cancer Institute of Canada. We also thank Janet Koprivnikar and Lisa Yu, who prepared the microCT specimens. R. Mark Henkelman is the recipient of a Canada Research Chair in Imaging.

REFERENCES

[1]Bassingthwaighte, J. B., L. S. Liebovitch, and B. J. West. Fractal Physiology. Oxford: Oxford University Press for the American Physiological Society, 1994.

[2]Gafiychuk, V. V., and I. A. Lubashevsky. On the principles of the vascular network branching. *J. Theor. Biol.* 212:1–9, 2001. doi:10.1006/jtbi.2001.2277.
[3]Kassab, G. S., C. A. Rider, N. J. Tang, and Y. C. Fung. Morphometry of pig coronary arterial trees. *Am. J. Physiol.* 265:H350–H365, 1993.
[4]Marxen, M. Fractal characteristics of vascular structure and modeling of blood flow in three dimensions. Ph.D. thesis, University of Toronto, 2005.
[5]Marxen, M., and R. M. Henkelman. Branching tree model with fractal vascular resistance explains fractal perfusion heterogeneity. *Am. J. Physiol. Heart Circ. Physiol.* 284:H1848–H1857, 2003.
[6]Marxen, M., J. G. Sled, L. X. Yu, C. Paget, and R. M. Henkelman. Comparing microsphere deposition and flow modeling in 3D vascular trees. *Am. J. Physiol. Heart Circ. Physiol.* 291:H2136–H2141, 2006. doi:10.1152/ajpheart.00146.2006.
[7]Marxen, M., M. M. Thornton, C. B. Chiarot, G. Klement, J. Koprivnikar, J. G. Sled, and R. M. Henkelman. Micro CT scanner performance and considerations for vascular specimen imaging. *Med. Phys.* 31:305–313, 2004. doi:10.1118/1.1637971.
[8]Mauroy, B., M. Filoche, E. R. Weibel, and B. Sapoval. An optimal bronchial tree may be dangerous. *Nature* 427:633–636, 2004. doi:10.1038/nature02287.
[9]Murray, C. D. The physiological principle of minimum work. I. The vascular system and the cost of blood volume. *Proc. Natl. Acad. Sci. USA* 12:207–214, 1926. doi:10.1073/pnas.12.3.207.
[10]Nordsletten, D. A., S. Blackett, M. D. Bentley, E. L. Ritman, and N. P. Smith. Structural morphology of renal vasculature. *Am. J. Physiol. Heart Circ. Physiol.* 291:H296–H309, 2006. doi:10.1152/ajpheart.00814.2005.
[11]Pallone, T. L., A. Edwards, and M. S. Kreisberg. The intrarenal distribution of blood flow. In: The Renal Circulation, edited by W. P. Anderson, R. G. Evans, and K. M. Stevenson. Stamford, CT: Jai Press Inc., 2000, pp. 75–92.
[12]Popel, A. S. Network models of peripheral circulation. In: Handbook of Bioengineering, edited by R. Skalak and S. Chien. New York: McGraw-Hill, 1987, pp. 201–2024.
[13]Press, W. H., B. P. Flannery, S. A. Teukolsky, and W. T. Vetterling. Numerical Recipes in C: The Art of Scientific Computing. Cambridge/New York: Cambridge University Press, 1992.
[14]Pries, A. R., T. W. Secomb, and P. Gaehtgens. Biophysical aspects of blood flow in the microvasculature. *Cardiovasc. Res.* 32:654–667, 1996.
[15]Sled, J. G., M. Marxen, and R. M. Henkelman. Analysis of micro-vasculature in whole kidney specimens using micro-CT. In 49th Annual Meeting of the International Symposium on Optical Science and Technology. *Proc. SPIE* 5535:53–64, 2004. doi:10.1117/12.559731.
[16]Strahler, A. N. Quantitative analysis of watershed geomorphology. *Trans. Am. Geophys. Union* 38:913–920, 1957.
[17]Suwa, N., and T. Takahashi. Morphological and Morphometrical Analysis of Circulation in Hypertension and Ischemic Kidney. Munich: Urban and Schwarzenberg, 1971.
[18]West, G. B., J. H. Brown, and B. J. Enquist. A general model for the origin of allometric scaling laws in biology. *Science* 276:122–126, 1997. doi:10.1126/science.276.5309.122.
[19]Xu, L. X., K. R. Holmes, B. Moore, M. M. Chen, and H. Arkin. Microvascular architecture within the pig kidney cortex. *Microvasc. Res.* 47:293–307, 1994. doi:10.1006/mvre.1994.1023.